Zero-Quantized Inter DCT Coefficient Prediction for Real-Time Video Coding

Jin Li, Moncef Gabbouj, *Fellow, IEEE,* and Jarmo Takala, *Senior Member, IEEE*

***Abstract*—Several algorithms were proposed to predict the zero-quantized DCT coefficients and reduce the computational complexity of transform and quantization. It is observed that these prediction algorithms achieve good performance for all-zero-quantized DCT blocks. However, the efficiency is much lower for non-all-zero-quantized DCT blocks. This paper proposes an algorithm to improve the prediction efficiency for non-all-zero-quantized DCT blocks. The proposed method extends the prediction to 1-D transforms by developing new Gaussian distribution based thresholds for 1-D transformation. Moreover, the proposed algorithm can perform the prediction on 1-D transforms in both the pixel domain and the transform domain. The prediction for the first stage of 1-D transforms is performed in the pixel domain. However, the second stage of 1-D transforms is performed in the 1-D DCT domain. Because after the first stage of 1-D transforms most energy is concentrated to a few low frequency 1-D DCT coefficients, many transforms in the second stage are skipped. Furthermore, the method fits well the traditional row and column transform structure, and it is more implementation friendly. Simulation results show that the proposed model reduces the complexity of transform and quantization more efficiently than competing techniques. In addition, it is shown that the overall video quality achieved by the proposed algorithm is comparable to the references.**

***Index Terms*—Computational complexity, DCT, quantization, real-time encoding, video coding.**

I. Introduction

TRADITIONALLY, high compression efficiency is usually achieved at the expense of increasing complexity. As the newest standard, H.264/AVC [1] significantly outperforms previous video codecs in terms of coding efficiency; its computational complexity is however greatly increased. The high complexity limits its application on mobile devices with low computation power as well as the real-time performance of the encoder. Currently, the emerging standard HEVC [2] claims an aggressive goal to reduce the encoding complexity by 50% compared to H.264/AVC high profile.

So far, many algorithms have been developed for fast discrete cosine transform calculation (e.g., [3]–[6]). These algorithms can be classified into two categories: direct and indirect algorithms. In 1991, Kou *et al*. [3] proposed a direct computation method that slightly reduces the number of multiplications and additions. On the other hand, indirect algorithms exploit the relationship between DCT and other transforms to reduce complexity. These algorithms include the calculations of DCT through the Hartley transform [4], polynomial transform [5], and paired transform [6]. Currently, many fast algorithms for multi-dimensional DCT computation are also emerging [7]–[10]. However, these algorithms still contain redundant computations as they do not take into account zero-quantized DCT (ZQDCT) coefficients.

When reducing redundant computations due to the ZQDCT coefficients, two types of prediction methods are considered: the prediction for the ZQDCT coefficients of intra blocks and the prediction of the residual pixel blocks. Nishida proposed a zero-value prediction for fast DCT calculation in [11]. If consecutive zero elements are produced during the DCT operation, the remaining transform and quantization are skipped. This method can be directly applied to the DCT and quantization. Although it reduces the total computations of DCT by 29% and quantization by 59% when applied to MPEG-2, the video quality is degraded by 1.6 dB on the average. In [12], we proposed a sufficient condition based prediction method for intra DCT and quantization to speed up the encoding process without video quality degradation. Later on, the complexity was further reduced at the cost of negligible video quality degradation in [13] and [14].

However, as inter DCT accounts for most of the discrete cosine transforms compared to intra DCT, complexity reduction regarding inter DCT has more significant impacts on improving the real-time performance. In the following, we will describe the state-of-the-art methods and how our proposed method is different from those solutions.

It is believed that motion compensated video frames are mainly composed of edge information of the original frames and could be well modeled by a Laplacian distribution. In [15], Pao *et al.* proposed a Laplacian distribution based model for the prediction of ZQDCT coefficients. Based on this model, an adaptive method with multiple thresholds is mathematically developed to reduce the computations of DCT, quantization, inverse quantization and inverse DCT in a video encoder. The

Manuscript received November 4, 2010; revised March 8, 2011 and May 29, 2011; accepted June 8, 2011. Date of publication June 27, 2011; date of current version February 8, 2012. This work was supported in part by the Project 213462 of the Academy of Finland [Finnish Center of Excellence Program (2006–2011)], by the Academy of Finland, under Grant 117065, and by the National Natural Science Foundation of China, under Grant 609111301281. This paper was recommended by Associate Editor R. Hamzaoui.

J. Li is with Panasonic, Singapore (e-mail: jin.li@tut.fi).

M. Gabbouj is with the Department of Signal Processing, Tampere University of Technology, Tampere 33101, Finland (e-mail: moncef.gabbouj@tut.fi).

J. Takala is with the Department of Computer Systems, Tampere University of Technology, Tampere 33101, Finland (e-mail: jarmo.takala@tut.fi).

Color versions of one or more of the figures in this paper are available online at http://ieeexplore.ieee.org.

Digital Object Identifier 10.1109/TCSVT.2011.2160749

8×8 DCT is simplified into three types of computation by comparing against the thresholds: no computation, 4×4 low frequency coefficients only and all the 64 DCT coefficients. As a result, the computations are reduced at the expense of 0.1–0.2 dB of video quality degradation in H.263.

Docef *et al.* [16] proposed a quantized DCT method that embeds the quantization into the DCT operations, where the computational complexity is reduced at the cost of negligible precision loss in computing the DCT. This method is particularly suitable for inter DCT of residual pixels where uniform quantization is applied. Experiments show that computational savings up to 60% of DCT and quantization are obtained for MPEG-2 and H.263. However, it results in 0.3–0.5 dB loss of objective video quality, rendering the visual quality somewhat objectionable.

Kim *et al.* [17] proposed new rate-quantization models for H.264/AVC to detect all-zero-quantized DCT blocks. In 2005, an improved detection algorithm [18] was proposed to reduce the complexity of H.264/AVC. However, it is only applicable to all-zero-quantized DCT blocks. A Gaussian distribution based model [19] was proposed in 2006 to predict the ZQDCT coefficients for fast video encoding. By using the same implementation method as in [15] comparable results are achieved by the Gaussian based thresholds based on XVID codec. When these prediction methods were applied to H.264/AVC in [20] and [21], good computational savings were also obtained. In 2007, the Gaussian distribution based model was optimized in [22] to further reduce the redundant computations for inter transform and quantization. A general method for detecting all-zero-quantized DCT blocks prior to DCT and quantization was proposed for H.264/AVC by Xie *et al.* in [23]. Using this model a number of computations for the all-zero-quantized DCT block are skipped. However, this method is limited to predict all-zero-quantized DCT blocks.

The previous methods can reduce the complexity of inter DCT and quantization, particularly for all-zero-quantized DCT blocks. However, since the DCT is usually implemented in a row and column structure, the efficiency of these algorithms is in practice highly lowered for non-all-zero-quantized DCT blocks. For instance, if the first 4×4 residual pixels are predicted as non-ZQDCT coefficients after quantization within an 8×8 block, only four 8-point 1-D transforms can be saved according to [15], [19], and [22] using the implementation structure in XVID codec, even though the other 48 DCT coefficients have been directly recognized as zeros. Although pruned DCT may reduce the complexity more, it requires multiple transform modules for hardware implementation.

Moreover, another drawback in the Laplacian and Gaussian thresholds exists in the prediction of ZQDCT coefficients for the non-all-zero-quantized DCT blocks. Since the thresholds are symmetric along the diagonal line from the top-left to the bottom-right, the prediction results also have a symmetric property when uniform quantization is applied for transforms in inter frames. For example, if the third DCT coefficient on the first row in a residual block is recognized as a non-zero value, the third coefficients on the first column are also predicted as a non-zero value. However, this is not always the case. Therefore, it is of great importance to develop such methods, which are able to efficiently predict the ZQDCT coefficients in the non-all-zero-quantized DCT blocks for further reduction.

Ji *et al.* extended the prediction for ZQDCT coefficients from the all zero-quantized DCT blocks to partially zero-quantized DCT blocks in accordance with the butterfly implementation structure in [24]. For non-all-zero-quantized DCT blocks, a fast transform algorithm is developed to determine the all zero-quantized DCT row or column and skip the calculations for those 1-D transforms by pruning the conventional butterfly based algorithms. This approach is developed based on the sufficient conditions at different frequency positions in the 8×8 DCT block. That is, each threshold is determined by the theoretical maximum value at a specific frequency position. This approach does not result in variation in terms of video quality. However, it only considers two cases for 1-D transform saving, i.e., the case of two 1-D transforms (columns 0 and 4) simultaneously skipped and the case of five 1-D transforms (columns 0, 4 and rows 0, 4, 2, or 6) simultaneously skipped in an 8×8 DCT block. All the other possibilities are just neglected. Therefore, the prediction efficiency is limited.

In this paper, we propose an improved prediction method to reduce the complexity of transform and quantization for non-all-zero-quantized DCT blocks. Different from previous techniques, the proposed algorithm extends the prediction from the pixel domain to the transform domain for 1-D transforms. Prediction is performed on both row and column transforms. At the first stage of row transform, the prediction is performed in the pixel domain. However, at the second stage of column transform, the prediction is performed in the transform domain, i.e., 1-D DCT domain. After the first stage of row transform, most energy is concentrated into a few low frequency coefficients. When the second stage of transform is performed, most computations regarding the columns only containing high frequency 1-D DCT coefficients are skipped. This advantage is particularly obvious at high bitrates. In addition, this algorithm lends itself to the butterfly implementation structure commonly used in video coding. In addition, the experimental results show a comparable video quality to the original codec by the proposed model.

In summary, the proposed algorithm improves the prediction efficiency for non-zero-quantized DCT blocks by extending the prediction to transform domain. The prediction is particularly efficient for the second stage of 1-D transforms because of the energy concentration in the first stage of 1-D transforms. The complexity reduction cause by the proposed algorithm is particularly obvious at high bitrate.

The rest of this paper is organized as follows. The Gaussian distribution based prediction for the all-zero-quantized DCT block is briefly reviewed in Section II. In Section III, a new Gaussian distribution based vector for non-all-zero-quantized DCT blocks is developed and implemented in accordance with the row and column transform structure. The experimental results and discussions are presented in Section IV. Finally, Section V concludes this paper.

II. Gaussian Prediction for N × N 2-D DCT

The 2-D DCT of a $N \times N$ data block $\boldsymbol{F}$ is defined in matrix form as

$$\boldsymbol{F} = \boldsymbol{A f A^T} \quad (1)$$

where $\boldsymbol{F}$ is the $N \times N$ matrix in DCT domain and the elements of the DCT matrix $\boldsymbol{A} = \{A[i, j]\}$ are

$$A[i, j] = \begin{cases} \dfrac{1}{\sqrt{N}} & i = 0,\ 0 \le j < N \\ \sqrt{\dfrac{2}{N}} \cos \dfrac{(2j+1)i\pi}{2N} & 1 \le i < N,\ 0 \le j < N. \end{cases}$$

Practically, N is selected as a power-of-two.

The experiments show that the distribution of the residual pixel $f(x, y)$ can be well modeled by Gaussian distribution with a significant peak at zero. In the following, a brief description of [19] is given with extension to the $N \times N$ DCT computations.

SAD is defined as the sum of absolute difference in a $N \times N$ residual block as

$$SAD = \sum_{X=0}^{N-1} \sum_{y=0}^{N-1} |f(x, y)|. \quad (2)$$

Since the residual pixel $f(x, y)$ is approximated by a Gaussian distribution with zero mean and the variance σ, we obtain

$$\sigma \approx \sqrt{\frac{\pi}{2}} \frac{SAD}{N^2}. \quad (3)$$

As the residual pixels have a zero mean value, the variance of the (u, v)th DCT coefficient can be expressed as

$$\sigma_F^2(u, v) = \sigma^2 [\boldsymbol{ARA^T}]_{u,u} [\boldsymbol{ARA^T}]v, v \quad (4)$$

where $\boldsymbol{A}$ is the matrix in (1) and $[\cdot]_{u,u}$ is the *(u, u)*th component of a matrix. The matrix $\boldsymbol{R}$ is defined as [25]

$$\boldsymbol{R} = \begin{bmatrix} 1 & \rho & \cdots & \rho^{N-1} \\ \rho & 1 & \cdots & \rho^{N-2} \\ \vdots & \vdots & \ddots & \vdots \\ \rho^{N-1} & \rho^{N-2} & \cdots & 1 \end{bmatrix}$$

and in this paper, the parameter ρ is selected according to [15], [19], and [22] as $\rho = 0.6$.

From (2), (3), and (4), a criterion for the ZQDCT coefficient with high probability [19] is derived with the parameter γ as

$$SAD < \beta_G(u, v) \alpha Q_p \quad (5)$$

where α represents the mapping relationship between the quantization parameter Q_p and the quantization step and

$$\beta_G(u, v) = \frac{\sqrt{2} N^2}{\gamma \sqrt{\pi [\boldsymbol{ARA}^T] u, u [\boldsymbol{ARA}^T] v, v}}. \quad (6)$$

Based on the above analysis, the Gaussian distribution based model with multiple thresholds is developed to reduce the inter DCT and quantization computations. For $N = 8$, the Gaussian distribution based thresholds β_G can be found in Table I in [19].

However, efficient prediction of individual ZQDCT coefficients does not necessarily result in good computational savings in practice. Since the 2-D DCT is usually implemented in the row and column structure in video coding, the Gaussian distribution based prediction does not work efficiently if the residual pixel block is regarded as a non-all-zero-quantized DCT block. Take $N = 8$ for example, if $\beta_G(2, 2)\alpha Q_p < SAD < \beta_G(5, 0)\alpha Q_p$ as shown in Fig. 1 where the quantization $aQ_p = 5$, $\beta_G(2, 2) = 15.51$ and $\beta_G(5, 0) = 16.46$, totally 49 DCT coefficients are predicted as zero-quantized values and can be directly set to zeros without the transform and quantization as shown in Fig. 2. However, since the 2-D DCT coefficients are not computed individually in practical implementation, only three 1-D transforms can be saved out of the total 16 1-D transforms. In other words, the saving is only 3/16 instead of 49/64 of the required DCT computations for this residual block. In addition, since the thresholds are symmetric along the diagonal line from the top-left to the bottom-right as shown in [19, Table I], the prediction results regarding the non-ZQDCT coefficients also have a symmetric property as shown in Fig. 2, which is not always the case.

TABLE I
Threshold $\beta(u)$ of 8-Point 1-D DCT

1.82	2.38	3.05	3.91	4.72	5.42	5.95	6.28

1	0	0	0	0	–1	–1	–1
–1	–1	–1	0	0	–1	1	0
0	1	0	0	0	2	1	1
0	0	0	0	0	0	0	1
–2	–2	–2	–2	–1	–1	–2	–1
–1	0	–1	0	1	1	1	0
–2	–1	–1	0	0	0	1	2
7	11	11	7	2	1	–1	–1

Fig. 1. Residual pixel block in 4CIF *City* sequence where $SAD = 81$.

N	N	N	N	N	Z	Z	Z
N	N	N	N	Z	Z	Z	Z
N	N	N	Z	Z	Z	Z	Z
N	N	Z	Z	Z	Z	Z	Z
N	Z	Z	Z	Z	Z	Z	Z
Z	Z	Z	Z	Z	Z	Z	Z
Z	Z	Z	Z	Z	Z	Z	Z
Z	Z	Z	Z	Z	Z	Z	Z

Fig. 2. Prediction based on the Gaussian thresholds, N denotes the 2-D DCT coefficient predicted as non-ZQDCT coefficient and Z represents the predicted ZQDCT coefficient.

III. Proposed Prediction for N-Point 1-D DCT

Preliminary work on the quantized DCT is presented in [16]. The main idea is to pre-compute and store a set of coefficients for each quantizer used in the encoder. For the case of uniform quantization, one QDCT routine is designed for each possible value of the quantization step. This effectively replaces the need for computing power by a small additional memory.

From (1), and (4) in [19], the QDCT coefficient $F^q(u, v)$ of the residual pixel $f(x, y)$ could be directly expressed as

$$\boldsymbol{F^q} = \boldsymbol{A^q f A^{qT}} \quad (7)$$

where

$$\boldsymbol{A}^{\boldsymbol{q}} = \frac{\boldsymbol{A}}{\sqrt{\alpha Q_p}}. \tag{8}$$

Therefore, the QDCT coefficient $F^q(u, v)$ will be rounded to zero if the following condition holds:

$$|F^q(u, v) < 1|. \tag{9}$$

Compared to the conventional separate transform and quantization, intermediate transaction for 1-D DCT coefficients may result in PSNR loss at the decoding side, particularly for integer computations. In [16], experiments on MPEG-2 and H.263 show that the QDCT algorithm has a little lower PSNR performance, but the degradation is negligible in practice. In this paper, the QDCT algorithm is only employed to justify the following proposed Gaussian prediction for the residual block recognized as non-all-zero-quantized DCT block and not initialized for the real implementation of the transform and quantization.

A. Proposed Prediction on the Row Transform

In accordance with the implementation structure of DCT in video coding, we propose a new prediction method on each row and column transformation for the residual pixel block identified as non-all-zero-quantized DCT block. In this paper, the DCT is supposed to be implemented in the row and column order.

Without the residual pixels in the all-zero-quantized DCT blocks, experimental results on several QCIF, CIF, and 4CIF sequences show that the remaining residual pixels in the non-all-zero-quantized DCT blocks still fit well the Gaussian distribution. Fig. 3. shows the distribution of these residual pixels and the ideal Gaussian distribution with zero mean. To facilitate the comparison between the ideal Gaussian distribution and the distribution of residual pixels, the amplitudes of all the curves are normalized to 1.

Similar to the Gaussian distribution based model in Section II, a new Gaussian prediction method could be developed in the same way for the 2-D QDCT of the residual pixel blocks. From (4) and (8), the variance of the (u, v)th quantized DCT coefficient $F^q(u, v)$ is expressed as

$$(\sigma_F^q)^2(u, v) = \sigma^2[\boldsymbol{A}^{\boldsymbol{q}}\boldsymbol{R}\boldsymbol{A}^{\boldsymbol{q}\boldsymbol{T}}]_{u,u}[\boldsymbol{A}^{\boldsymbol{q}}\boldsymbol{R}\boldsymbol{A}^{\boldsymbol{q}\boldsymbol{T}}]_{v,v}. \tag{10}$$

With the same definition of SAD in (2), the DCT coefficient $F(u, v)$ will be truncated to zero with a high probability if

$$SAD < \beta_g^q(u, v) \tag{11}$$

where

$$\boldsymbol{\beta}_{\boldsymbol{G}}^{\boldsymbol{q}} = \frac{\sqrt{2}N^2}{\gamma\sqrt{\pi[\boldsymbol{A}^{\boldsymbol{q}}\boldsymbol{R}\boldsymbol{A}^{\boldsymbol{q}^T}]_{u,u}[\boldsymbol{A}^{\boldsymbol{q}}\boldsymbol{R}\boldsymbol{A}^{\boldsymbol{q}\boldsymbol{T}}]_{v,v}}}. \tag{12}$$

The Gaussian distribution based matrix $\boldsymbol{\beta}_{\boldsymbol{G}}^{\boldsymbol{q}}$ can be further decomposed as follows:

$$\boldsymbol{\beta}_{\boldsymbol{G}}^{\boldsymbol{q}} = \boldsymbol{\beta}^{\boldsymbol{q}}\boldsymbol{\beta}^{\boldsymbol{q}\boldsymbol{T}} \tag{13}$$

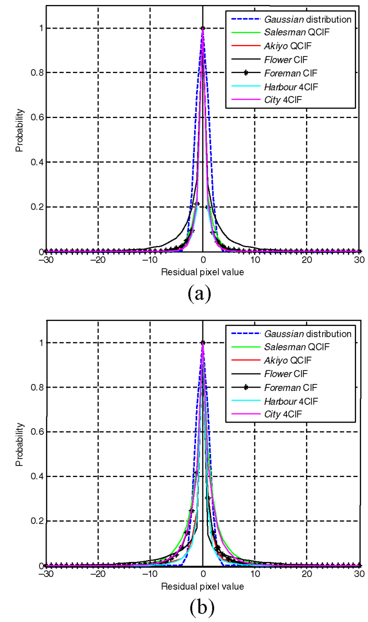

Fig. 3. Distribution of the residual pixels $f(x, y)$ of non-all-zero-quantized blocks in seven video sequences at (a) $Q_p = 4$ and (b) $Q_p = 24$. All the curves are normalized.

where $\boldsymbol{\beta}^{\boldsymbol{q}}$ is a vector and with (8) the uth element of $\boldsymbol{\beta}^{\boldsymbol{q}}$ is defined as

$$\beta^q(u) = \beta(u)\sqrt{\alpha Q_p}, \qquad u = 0, 1, \ldots, N-1 \tag{14}$$

where

$$\beta(u) = \sqrt[4]{\frac{2}{\pi}\frac{N}{\sqrt{\gamma|[\boldsymbol{A}\boldsymbol{R}\boldsymbol{A}^{\boldsymbol{T}}]_{u,u}|}}}.$$

As the discrete cosine transform is also an orthogonal transform, 2-D transform can be implemented with separate row and column transforms, thus the prediction for the ZQDCT coefficients can be performed on each row and each column transform by comparing the sum of absolute difference $SAD^r(y)$ and the thresholds for each row. If $SAD^r(y)$ is defined as

$$SAD^r(y) = \sum_{x=0}^{N-1} |f(x, y)| \qquad y = 0, 1, \ldots, N-1 \tag{15}$$

where y refers the yth row in a $N \times N$ block. Therefore, similar to the Gaussian prediction for 2-D DCT, the 1-D DCT coefficient $F(u, y)$ will be regarded as zero if the following condition holds:

$$SAD^r y < \beta(y)\sqrt{\alpha Q_p} \quad u, y = 0, 1, \ldots, N-1 \tag{16}$$

where u indicates the uth element in the prediction vector $\boldsymbol{\beta}$ for each row transform.

Based on the above analysis, a new prediction vector based on the Gaussian distribution is developed to detect the ZQDCT coefficients on the row transform. For example, if $SAD^r(y) < \beta(0)\sqrt{\alpha Q_p}$, all the DCT coefficients regarding this row transform will be predicted as zeros, thus all the

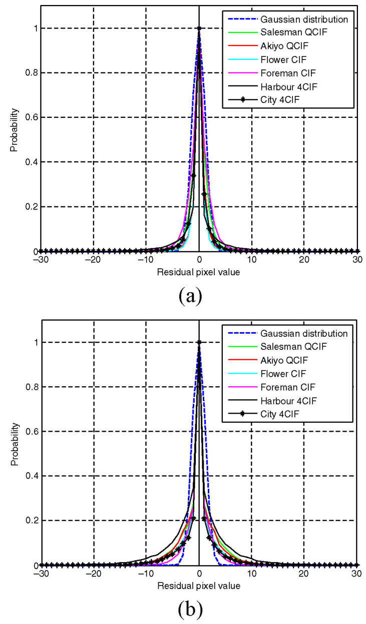

Fig. 4. Distribution of the 1-D DCT coefficients $F(u, v)$ of non-all-zero-quantized DCT blocks at (a) $Q_p = 4$ and (b) $Q_p = 24$. All the curves are normalized.

computations can be omitted. Otherwise, we compute the transform based on the original transform structure.

As stated in [16], additional quality distortion is introduced due to the immediate transaction by embedding the quantization into the 1-D DCT. On the other hand, a stricter threshold can prevent the decrease of quality distortion. Therefore, a higher value of γ in (12) is selected here for the prediction of 1-D DCT coefficients and presenting a compromise between the prediction efficiency and the introduced distortion. For $N = 8$, $\gamma = 5$, the thresholds are shown in Table I.

B. Proposed Prediction on the Column Transform

Before applying the new prediction vector based on the Gaussian distribution to the column transform, experiments on various sizes of sequences are carried out to further show that the distribution of the 1-D DCT coefficients after the row transform still follows a Gaussian distribution with zero mean similarly to Fig. 3, shown as Fig. 4.

Since the 1-D DCT coefficients in non-all-zero-quantized row are not really quantized, the same quantization should be applied to the 2-D DCT coefficients after the column transform. Therefore, a new criterion can be directly calculated based on the same strategy as the prediction for the row transform as

$$SAD^c(u) < \beta(v)\alpha Q_p \qquad u, v = 0, 1, \ldots, N-1 \tag{17}$$

where

$$SAD^c(u) = \sum_{y=0}^{N-1} |F(u, v)| \quad u = 0, 1, \ldots, N-1$$

and u refers the uth column in a $N \times N$ block and v indicates the vth element in the prediction vector β for each column transform.

TABLE II
HYBRID THRESHOLDS FOR THE 8-POINT 1-D DCT

2.83	2.38	3.05	3.91	4.72	5.42	5.95	6.28

Compared to the thresholds in the row transform stage, the difference in the following column transform is the quantization parameter Q_p. As no quantization is actually introduced during the first transform stage, the 2-D DCT coefficients should be fully quantized. Therefore, the thresholds are calculated based on the parameter αQ_p.

It is worth pointing out that the row and column transforms are actually equivalent in the proposed model. The difference is the comparison thresholds. According to [16], squared uniform quantization, i.e., $\sqrt{\alpha Q_p}$ in (8), could be embedded into 1-D transforms for inter frames. In the proposed model, the thresholds for the first stage of 1-D transforms are computed from the squared quantization, but the 1-D DCT coefficients are not really quantized if the 1-D transform is not predicted as all-zero-quantized-row. The purpose is to limit the possible precision loss only to the predicted ZQDCT coefficients in the all-zero-quantized-row and has no effect on the other 1-D DCT coefficients Therefore, for the second stage of 1-D transforms, the thresholds should be computed from the original quantization, i.e., αQ_p, and the 2-D DCT coefficients should be quantized with αQ_p.

C. Optimization of the Proposed Algorithm

The range of DCT coefficients has been analytically studied in previous work [12], [13], and [22]. Comprehensive analysis on H.264/AVC can be found in [20] and [21]. For a $N \times N$ block, the 2-D DCT coefficients $F(u, v)$ will be zero if

$$SAD < \frac{N\alpha Q_p}{2c(u)c(v)\max\left\{|\cos\frac{(2x+1)u\pi}{2N}||\cos\frac{(2y+1)v\pi}{2N}|\right\}}. \tag{18}$$

From (18), the DCT coefficients can be bounded depending on the frequency position that affects the maximum values of the two cosine functions. As a result, the sufficient condition based thresholds $\beta_s(u, v)$ that determine whether the quantized DCT coefficients to be zero-valued are derived. It is worth pointing out that as the thresholds are mathematically derived from the ideal maximum value of the DCT coefficients, i.e., based on the sufficient condition, it does not lead to any quality degradation compared to the traditional transform method.

According to the analysis of DCT coefficients, we find out that the Gaussian distribution based thresholds $\boldsymbol{\beta_G}$ can be further improved by combining the sufficient condition based thresholds $\boldsymbol{\beta_S}$. The new thresholds $\boldsymbol{\beta_{2D}}$ are determined by selecting the larger one between $\beta_G(u, v)$ and $\beta_S(u, v)$ as

$$\beta_{2D}(u, v) = \max(\beta_G(u, v), \beta_S(u, v)) \qquad 0 \le u, v < N. \tag{19}$$

Take $N = 8$ for example, the first threshold for DC term, i.e., 5.54 in Table I in [19], is replaced with the threshold of 8.00.

TABLE III
MAIN STEPS FOR THE RESIDUAL PIXEL BLOCK ($u, v = 0, 1, \ldots, N-1$)

Condition	Type	DCT and Quantization
$SAD < \min(\beta_{2D}(u, v))\alpha Q_p$	The residual block is predicted as an all-zero-quantized DCT block	Not performed
$SAD \geq \min(\beta_{2D}(u, v))\alpha Q_p$	The block is predicted as a non-all-zero-quantized DCT block	Do the 2-D transform in the row and column structure
$SAD^r(u) < \min(\beta_{1D}(u, v))\sqrt{\alpha Q_p}$	The row is recognized as an all-zero-quantized row	Not performed
$SAD^r(u) \geq \min(\beta_{1D}(u, v))\sqrt{\alpha Q_p}$	The row is predicted to contain non-zero values	Do the row transform as normal
$SAD^c(u) < \min(\beta_{1D}(u, v))\alpha Q_p$	The column is predicted to have only zeros after quantization	Not performed
$SAD^c(u) \geq \min(\beta_{1D}(u, v))\alpha Q_p$	Predicted to contain non zeros after quantization	Do the transform and the following quantization as normal

For 1-D DCT on the row direction, the coefficient $F(u, y)$ on each row will be predicted as zero if

$$SAD^r(y) < \sqrt{\frac{N}{2}} \frac{Q'}{c(u) \max\left\{ \left| \cos \frac{(2x+1)u\pi}{2N} \right| \right\}} \tag{20}$$

where Q' is the quantization used to truncate the DCT coefficients. In this paper, Q' is defined as $\sqrt{\alpha Q_p}$ for the row transforms and αQ_p for the column transforms. Again, take $N = 8$ for example, the new hybrid thresholds $\boldsymbol{\beta_{1D}}$ by combining the Gaussian distribution based vector and the sufficient condition based prediction are computed and shown in Table II. The definition of $\boldsymbol{\beta_{1D}}$ is as $\boldsymbol{\beta_{2D}}$ in (19).

D. Summary of the Proposed Method

Given the above analysis, we propose a model to predict the ZQDCT coefficients for inter DCT and quantization by combining the Gaussian distribution based prediction and the sufficient condition based prediction. It is worth pointing out that since the calculations of SAD and $SAD^r(y)$ are linear, the overhead computations regarding SAD and $SAD^r(y)$ can be performed during motion estimation and motion compensation as done in [15], [19], and [22]. In this case, only additional comparisons are introduced. However, calculations of $SAD^c(u)$ require more additions for residual blocks identified as non-all-zero-quantized DCT blocks in the proposed algorithm. On other hand, the quantization Q_p is a constant value during the encoding process, thus the thresholds and the new transform matrix $\boldsymbol{A^q}$ are pre-computed prior to the DCT and quantization and stored for comparisons. In other words, we compute the thresholds and the new transform matrix only once in the whole encoding process. The main steps of the proposed method are summarized as follows.

1) The sums of absolute difference, SAD of the residual pixel block and $SAD^r(y)$ of the residual pixels in the row direction are first calculated. Then SAD is compared with the smallest threshold of $\beta_{2D}(u, v)$ where $u, v = 0, 1, \ldots, N-1$. If $SAD < \min(\beta_{2D}(u, v))\alpha Q_p$, the block is recognized as all-zero-quantized DCT block and the calculations for the DCT and quantization are skipped.
2) Otherwise, the residual block is predicted as a non-all-zero-quantized DCT block. Therefore, the row transform is carried out first and $SAD^r(y)$ is compared with the smallest threshold of $\beta_{1D}(u, v)$. If $SAD^r(y) < \min(\beta_{1D}(u, v))\sqrt{\alpha Q_p}$, it is predicted as an all-zero-quantized DCT row. Therefore, the coefficients are directly set to zeros without further computations. Otherwise, do the row transform based on the default structure in the codec.
3) For the column transform, the sum of absolute difference $SAD^c(u)$ of the 1-D DCT coefficients is calculated. If $SAD^c(u) < \min(\beta_{1D}(u, v))\sqrt{\alpha Q_p}$, all the 2-D DCT coefficients in this column are set to zeros without transform and quantization. Otherwise, do the transform and quantization normally.

Summary of the proposed method is given in Table III where the value Q_p is the quantization parameter and the parameter a denotes the mapping relationship between Q_p and the quantization value. The hybrid model only considers three types of DCT and quantization, which can be skipped: the 2-D DCT and the 1-D DCT on the row and column directions.

IV. EXPERIMENTAL RESULTS AND DISCUSSION

A. Experimental Results on XVID Codec

In order to evaluate the performance of the proposed model, a series of experiments were carried out, using C-code, based on XVID codec [26] against competing methods. Since XVID codec is designed for MPEG-4 Visual and H.263 where the 8×8 DCT is employed, we take $N = 8$ throughout the experiments. Four 4CIF sequences (*City*, *Crew*, *Harbor*, and *Soccer*) with a frame rate of 30 are used to report the results and 200 frames are used in the experiments for each sequence. The codec was compiled with Microsoft Visual Studio 2008.

1) *Comparisons of Video Quality:* First, the PSNR and bit rates are compared among the test modes with the original codec as shown in Table IV. Based on the experiments, all the methods result in video quality degradation, but meanwhile lower bit rates. Therefore, it is hard to conclude according to the results in Table IV.

In addition, the rate-distortion (R-D) performance is studied in the experiments, thus new conclusions are drawn. Fig. 5

TABLE IV
COMPARISONS OF AVERAGE PSNR (dB) AND BIT RATE (ΔR, %)

Image	Q_P	ΔPSNR (dB)				ΔR (%)				ΔENC (%)				
		Proposed	[19]	[22]	[15]	Proposed	[19]	[22]	[15]	Proposed	[22]	[19]	[15]	[24]
City	4	−0.05	−0.06	−0.05	−0.07	−0.21	−0.31	−0.30	−0.09	−3.63	−1.57	−1.05	−0.76	−0.92
	8	−0.06	−0.08	−0.09	−0.06	−0.04	−1.06	−1.06	−0.51	−7.95	−6.37	−5.10	−4.35	−5.43
	16	−0.03	−0.14	−0.11	−0.09	−0.17	−2.46	−2.39	−1.19	−10.04	−9.12	−7.65	−6.93	−8.01
	30	−0.04	−0.12	−0.06	−0.09	−0.10	−0.85	−1.08	−0.63	−12.39	−12.42	−11.25	−10.39	−11.31
Crew	4	−0.07	−0.07	−0.06	−0.05	−0.41	−0.02	−0.02	−0.02	−3.06	−0.33	−0.29	−0.18	−0.26
	8	−0.06	−0.04	−0.08	−0.08	−0.09	−0.05	−0.14	−0.07	−7.39	−5.42	−4.37	−4.05	−4.28
	16	−0.08	−0.05	−0.14	−0.11	−0.02	−0.06	−0.13	−0.03	−10.91	−10.08	−9.56	−8.93	−9.11
	30	−0.07	−0.09	−0.13	−0.09	−0.11	−0.07	−0.09	−0.04	−14.20	−14.03	−12.84	−11.73	−12.92
Harbor	4	−0.07	−0.02	−0.03	−0.04	−0.53	−0.07	−0.05	−0.02	−2.91	−1.25	−0.89	−0.62	−0.83
	8	−0.05	−0.09	−0.06	−0.07	−0.06	−0.19	−0.59	−0.09	−6.97	−4.29	−3.18	−2.90	−3.26
	16	−0.05	−0.08	−0.11	−0.09	−0.10	−0.72	−0.71	−0.41	−9.74	−6.89	−6.03	−5.72	−6.11
	30	−0.10	−0.11	−0.13	−0.15	−0.05	−0.61	−0.65	−0.38	−10.96	−10.62	−8.01	−7.32	−7.28
Soccer	4	−0.08	−0.09	−0.06	−0.06	−0.39	−0.10	−0.09	−0.05	−4.63	−1.63	−1.33	−0.87	−1.20
	8	−0.06	−0.08	−0.06	−0.03	−0.15	−0.17	−0.35	−0.09	−8.24	−6.01	−4.93	−4.52	−5.18
	16	−0.09	−0.11	−0.09	−0.01	−0.13	−0.57	−0.56	−0.21	−11.27	−10.57	−8.15	−7.43	−8.13
	30	−0.11	−0.15	−0.08	−0.08	−0.16	−0.31	−0.24	−0.14	−14.28	−14.12	−12.55	−11.07	−12.32
Average		−0.07	−0.09	−0.08	−0.07	−0.17	−0.48	−0.53	−0.25	−8.66	−7.17	−6.07	−5.49	−6.03

shows the comparisons between the test models and the original codec. Particularly, since [24] does not result in any prediction error, it has exactly the same video quality as the original codec. According to the results, all the other models also achieve comparable R-D performance to the original codec. In addition, based on the results in the magnified local areas it is hard to tell which model performs best in terms of video quality and each model is not necessarily better or worse than the others, which is different from the conclusion in many references stated as "negligible video quality degradation."

2) *Complexity Reduction on Arithmetic Numbers:* The default 2-D DCT in the XVID codec requires 12 multiplications and 32 additions for each 1-D transform [26]. All the overheads in the test models are taken into account for measurement. Since the calculations of sum of absolute values as SAD and $SAD^r(y)$ are linear, they can be pre-computed during motion estimation. Therefore, only one comparison is introduced if the residual block is identified as an all-zero-quantized DCT block in the four test models.

However, if the block is predicted as a non-all-zero-quantized DCT block, 56 additions and 16 comparisons more are introduced by the proposed model for calculations of $SAD^c(y)$ and prediction of the 1-D transforms. In [22], the number of overheads is 2 for non-all-zero-quantized DCT block. In [15] and [19], the numbers of comparisons are 2 for the DC term only and 3 for the others. In [24], the required overhead operations can be referenced in [24, Table III]. The complexity reduction is defined as

$$OP = \frac{OP_{rdct+q} + OP_{\text{overhead}}}{OP_{dct+q}} \times 100\% \qquad (21)$$

where OP_{rdct+q} denotes the required operation number of DCT and quantization in the test models, OP_{dct+q} is the total operation number of DCT and quantization in the original codec, and OP_{overhead} is the introduced overhead operations in the test models. The resulting statistics are shown in Fig. 6.

According to the results, the proposed method could save about 19.8%–91.3% of the transform and quantization computations and significantly outperforms the others at high bit rates in terms of operation number. In addition, it is observed that the numbers of overhead comparisons in the references are very small, ranging between 0.18% and 0.42%. On other hand, the proposed model requires more additional operations for calculation of non-all-zero-quantized DCT blocks than all-zero-quantized DCT blocks. At high bit rates, many blocks are predicted as non-all-zero-quantized DCT blocks and, therefore, lots of overhead operations are introduced. However, with increasing quantization more blocks are predicted as all-zero-quantized DCT blocks, thus the proposed model requires less overheads and the proportion in the overall complexity becomes smaller as shown in Fig. 6.

In addition, complexity reduction regarding executive time of the entire encoding process is compared among the test models against the reference XVID codec as shown in Table IV. The reduction is defined as

$$ENC = \frac{ENC_{\text{ref}} - ENC_{\text{test}}}{ENC_{\text{ref}}} \times 100\% \qquad (22)$$

where ENC_{ref} defines the encoding time required for the reference software and the ENC_{test} is the encoding time for the test models. According to the results, the proposed model achieves the best performance compared to other prediction methods. For example, the proposed method reduced 1.49% of the entire encoding time more than [22], the best one among the [15], [19], [22], [24] and the reference codec.

B. *Experiments on H.264/AVC Codec*

In addition, the reference software JM16.2 [27] is used to carry out experiments against the competing methods [18], [20], and [21] with the baseline profile. The transform in H.264/AVC operates on 4 × 4 blocks of residual data and is an approximation of DCT in order to avoid multiplications. That is, the "core" DCT transform is decomposed into a new

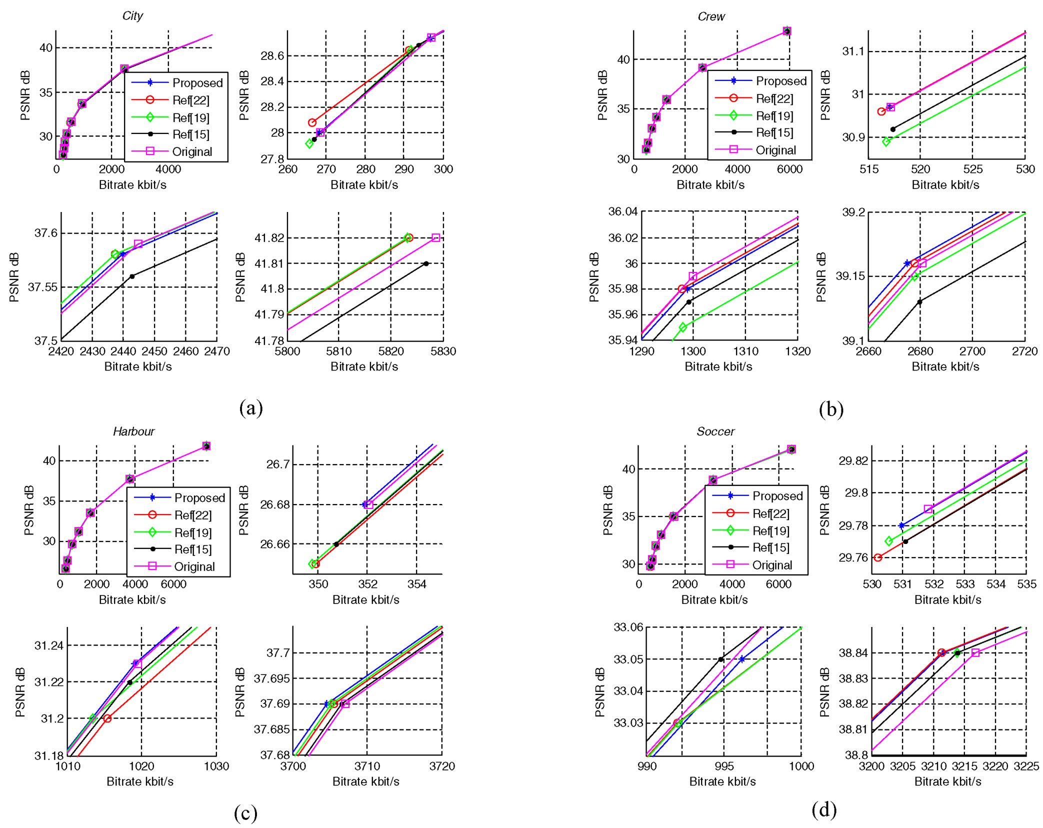

Fig. 5. Rate-distortion performance regarding luminance component on XVID codec between the test models and the original codec. (a) *City*. (b) *Crew*. (c) *Harbor*. (d) *Soccer*. Results for each sequence consist of an overall R-D performance and three locally magnified comparisons.

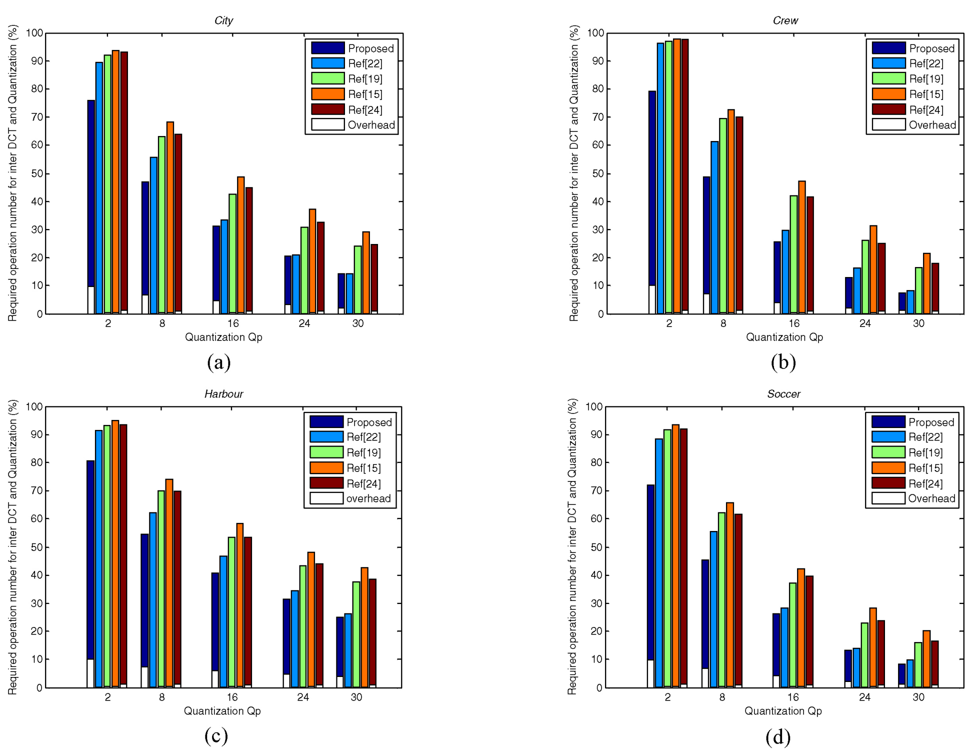

Fig. 6. Complexity reduction in terms of the number of arithmetic operation on XVID codec. (a) *City*. (b) *Crew*. (c) *Harbor*. (d) *Soccer*. Each bar is composed of two parts: the "WHITE" area means the overhead operations and the upper part only considers the DCT and quantization. Pruned DCT is used for [15], [19], and [22].

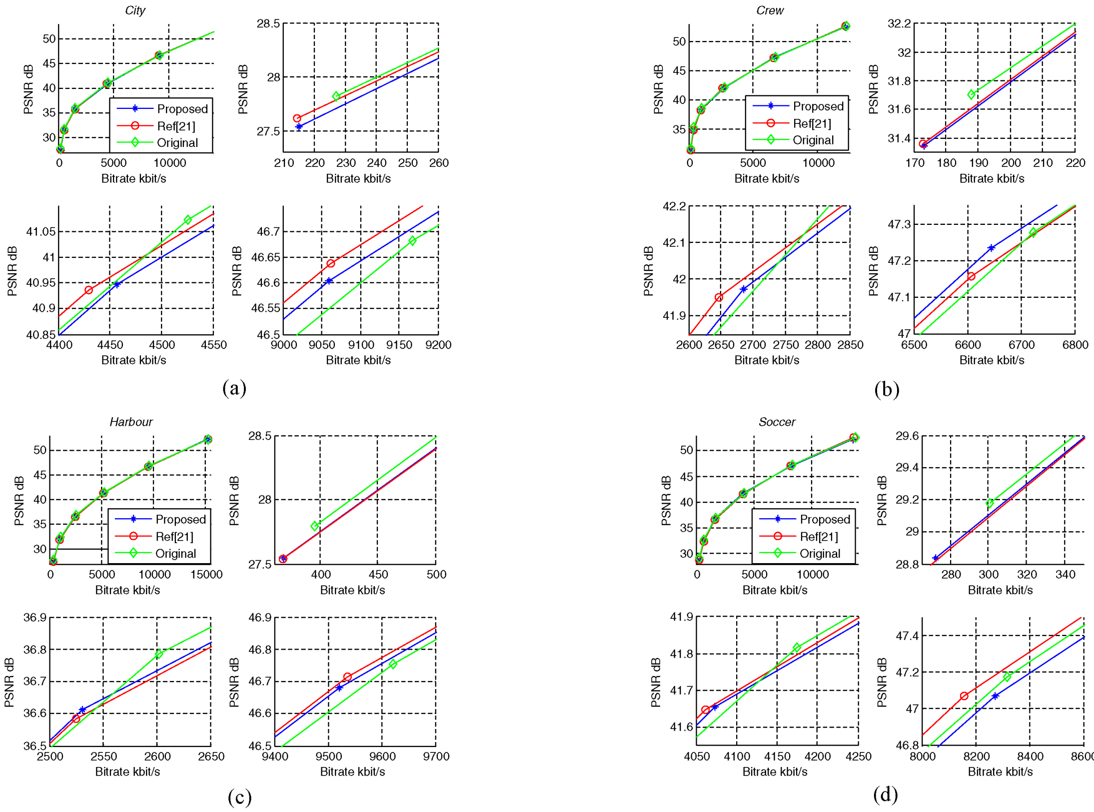

Fig. 7. Rate-distortion performance regarding luminance component on H.264. (a) *City*. (b) *Crew*. (c) *Harbor*. (d) *Soccer*. Each sequence consists of an overall comparison and three local comparisons.

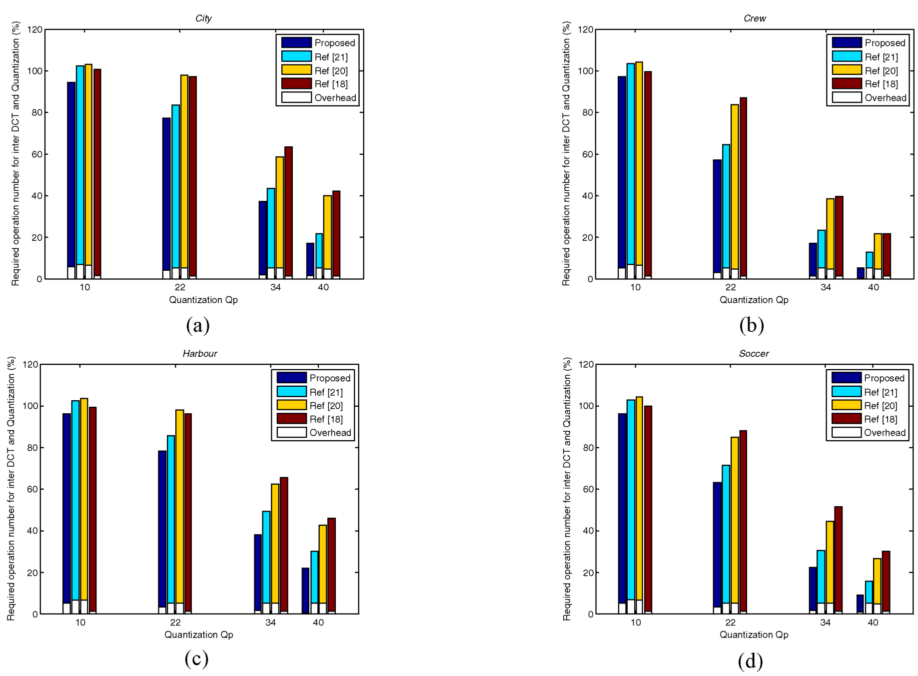

Fig. 8. Complexity reduction in terms of the number of arithmetic operations on H.264. (a) *City*. (b) *Crew*. (c) *Harbor*. (d) *Soccer*. Each bar is composed of two parts: the “WHITE” area means the overhead operations and the upper part only considers the DCT and quantization. Pruned DCT is used for [21].

"core" H.264 transform and a matrix of scaling factors, i.e., part of the DCT transform. However, since the scaling matrix is integrated into the following quantizer, the thresholds in the proposed method which are calculated from the "core" DCT transform matrix and the quantization are still justified. For $N = 4$, the thresholds $\min(\beta_{2D}(u, v))$ and $\min(\beta_{1D}(u, v))$, $0 \leq u, v < 4$, are 3.1397 and 1.8142, respectively.

The same experiments and evaluations are performed as on XVID codec. Fig. 7 shows the quality comparisons among the proposed approach and the references. Since [18] and [20] are proposed with the sufficient condition based thresholds, no degradation was observed in the experiments. According to the reported results, both the proposed approach and [21] generate noise-like variations in terms of objective video quality at the decoder, but the overall video qualities are still comparable to the reference codec.

Fig. 8 shows the reduction of operation number including additions, shifts, comparisons, and multiplications. Similar to the analysis on XVID codec, the proposed method requires one additional comparison for each all-zero-quantized DCT block and 21 operations (9 comparisons and 12 additions) for each non-all-zero-quantized DCT block. In addition, [18] and [20] required 5 and 23 overhead operations for each residual block, respectively. For [21], the number of overheads is between 23 and 26 depending on the types of different prediction. More details can be found in [21, Table IV].

The experiments show that the proposed method results in an average savings of 46.6% as shown in Fig. 8 and performs better than the references at both high bit rates and low bit rates. This is mainly due to additional overheads introduced by [20] and [21]. Although [20] and [21] tend to reduce more computations on transform and quantization than [18] at high bit rates, the overall complexity is even higher because of the additional overhead operations. Experimental results also show that [20] and [21] even require more computations than the original codec at very high bit rates, e.g., $Q_p = 10$.

Besides, tentative experiments were carried out on the HEVC HM2.0 codec. By applying the proposed scheme to HEVC, thresholds for different size of transform unit (TU) were developed. Experimental results show that most of the computational savings were achieved from large size TUs, i.e., 16×16 and 32×32. The reason is that large size TU is usually used in the areas containing small residuals such as the homogenous areas or areas with low motion activities. Thus, the large TUs are more likely predicted as all-zero-quantized DCT blocks or partially all-zero-quantized DCT blocks than small TUs.

V. Conclusion

An improved Gaussian based prediction is proposed to reduce the complexity of inter DCT and quantization. The proposed model extends the prediction from pixel domain to transform domain. Because most energy is concentrated into a few low frequency 1-D DCT coefficients after the first stage of 1-D transforms, most computations on the second stage of transforms are skipped. Experiments show that this proposed algorithm could more efficiently reduce the complexity for non-all-zero-quantized DCT blocks than competing techniques. This advantage is particularly obvious at high bit rates. In addition, the proposed algorithm is designed in accordance with the butterfly structure. Therefore, it is more implementation friendly for hardware. Experiments show that the proposed model reduces the computations for transform and quantization by 51.2% on average by summarizing the results on MPEG-4 and H.264. Although the proposed method results in an average of 0.12 dB degradation, the overall video quality is comparable to the reference codec because of the 6.6% bit rate decrease on average. The proposed method is particularly valuable in improving efficiency for low-power processors.

References

[1] H. Kalva, "The H.264 video coding standard," *IEEE Trans. Multimedia*, vol. 13, no. 4, pp. 86–90, Oct. 2006.

[2] *H265.net* [Online]. Available: http://www.h265.net

[3] W. Kou and T. Fjallbrant, "A direct computation of DCT coefficients for a signal block taken from two adjacent blocks," *IEEE Trans. Acoust. Speech Signal Process.*, vol. 39, no. 7, pp. 1692–1695, Jul. 1991.

[4] H. S. Malvar, "Fast computation of the discrete cosine transform through fast Hartley transform," *Electron. Lett.*, vol. 22, no. 7, pp. 352–353, 1986.

[5] P. Duhamel and C. Guillemot, "Polynomial transform computation of the 2-D DCT," in *Proc. IEEE Int. Conf. Acoust. Speech Signal Process.*, Apr. 1990, pp. 1515–1518.

[6] A. M. Grigoryan, "An algorithm for calculation of the discrete cosine transform by paired transform," *IEEE Trans. Signal Process.*, vol. 53, no. 1, pp. 265–273, Jan. 2005.

[7] Q. Dai, X. Chen, and C. Lin, "Fast algorithm for multidimensional DCT-to-DCT computation between A block and its associated sub-blocks," *IEEE Trans. Signal Process.*, vol. 53, no. 8, pp. 3219–3225, Aug. 2005.

[8] A. Elnaggar and H. M. Alnuweiri, "A new multidimensional recursive architecture for computing the discrete cosine transform," *IEEE Trans. Circuits Syst. Video Technol.*, vol. 10, no. 1, pp. 113–119, Feb. 2000.

[9] X. Chen, Q. Dai, and C. Li, "A fast algorithm for computing multidimensional DCT on certain small sizes," *IEEE Trans. Signal Process.*, vol. 51, no. 1, pp. 213–220, Jan. 2003.

[10] Z. Zhao, H. Chen, X. Wen, and A. Sang, "Real-time video compression based on three-dimensional matrix DCT," in *Proc. IEEE Int. Conf. Signal Process.*, Aug.–Sep. 2004, pp. 1155–1158.

[11] Y. Nishida, K. Inoue, and V. G. Moshnyaga, "A zero-value prediction technique for fast DCT computation," in *Proc. IEEE Workshop Signal Process. Syst.*, Aug. 2003, pp. 165–170.

[12] J. Li, J. Takala, M. Gabbouj, and H. Chen, "A detection algorithm for zero quantized DCT coefficients in JPEG," in *Proc. IEEE Int. Conf. Acoust. Speech Signal Process.*, Mar.–Apr. 2008, pp. 1189–1192.

[13] J. Li, M. Gabbouj, and J. Takala, "Hybrid modeling of intra DCT coefficients for real-time video encoding," *EURASIP J. Image Video Process.*, vol. 2008, no. 749172, pp. 1–13, 2008.

[14] J. Li, M. Gabbouj, J. Takala, and H. Chen, "Laplacian modeling for real-time encoding," in *Proc. IEEE Int. Conf. Multimedia Expo*, Jun. 2008, pp. 797–800.

[15] I. M. Pao and M. T. Sun, "Modeling DCT coefficients for fast video encoding," *IEEE Trans. Circuits Syst. Video Technol.*, vol. 9, no. 4, pp. 608–616, Jun. 1999.

[16] A. Docef, F. Kossentini, K. Nguuyen-Phi, and I. R. Ismaeil, "The quantized DCT and its application to DCT-based video coding," *IEEE Trans. Circuits Syst. Video Technol.*, vol. 11, no. 3, pp. 177–187, Mar. 2002.

[17] G. Y. Kim, Y. H. Moon, and J. H. Kim, "An early detection method of all-zero DCT blocks in H.264," in *Proc. IEEE Int. Conf. Image Process.*, Oct. 2004, pp. 453–456.

[18] Y. H. Moon, G. Y. Kim, and J. H. Kim, "An improved early detection algorithm for all-zero blocks in H.264 video coding," *IEEE Trans. Circuits Syst. Video Technol.*, vol. 15, no. 8, pp. 1053–1057, Aug. 2005.

[19] H. Wang, S. Kwong, and C. Kok, "Fast video coding based on Gaussian model of DCT coefficients," in *Proc. IEEE ISCAS*, May 2006, pp. 1073–1076.

[20] H. Wang, S. Kwong, and C. Kok, "Efficient prediction algorithm of integer DCT coefficients for H.264/AVC optimization," *IEEE Trans. Circuits Syst. Video Technol.*, vol. 16, no. 4, pp. 547–552, Apr. 2006.

[21] H. Wang and S. Kwong, "Hybrid model to detect zero quantized DCT coefficients in H.264," *IEEE Trans. Multimedia*, vol. 9, no. 4, pp. 728–735, Jun. 2007.

[22] H. Wang, S. Kwong, and C. W. Kok, "Efficient predictive model of zero quantized DCT coefficients for fast video encoding," *Image Vis. Comput.*, vol. 25, no. 6, pp. 922–933, 2007.

[23] Z. Xie, Y. Liu, J. Liu, and T. Yang, "A general method for detecting all-zero blocks prior to DCT and quantization," *IEEE Trans. Circuits Syst. Video Technol.*, vol. 17, no. 2, pp. 237–241, Feb. 2007.

[24] X. Ji, S. Kwong, D. Zhao, H. Wang, C.-C. J. Kuo, and Q. Dai, "Early determination of zero-quantized 8×8 DCT coefficients," *IEEE Trans. Circuits Syst. Video Technol.*, vol. 19, no. 12, pp. 1755–1765, Dec. 2009.

[25] A. K. Jain, *Fundamentals of Digital Image Processing*. Englewood Cliffs, NJ: Prentice-Hall, 1989.

[26] *Xvid Codec* [Online]. Available: http://www.xvid.org

[27] *H.264/AVC JM Reference Software* [Online]. Available: http://iphome.hhi.de/suehring/tml

Jin Li received the B.S. and M.S. degrees in technology and instrument of testing and control, and communication and information system from Jilin University, Changchun, China, in 2002 and 2005, respectively.

From October 2005 to February 2011, he was a Researcher with the Department of Signal Processing, Tampere University of Technology, Tampere, Finland. He is currently a Research Engineer with Panasonic, Singapore, contributing to the HEVC standardization. His current research interests include image/video coding, 3-D video processing, and image processing.

Moncef Gabbouj (F'11) received the B.S. degree in electrical engineering from Oklahoma State University, Stillwater, in 1985, and the M.S. and Ph.D. degrees in electrical engineering from Purdue University, West Lafayette, IN, in 1986 and 1989, respectively.

He is currently an Academy of Finland Professor with the Department of Signal Processing, Tampere University of Technology, Tampere, Finland. He was the Head of the department from 2002 to 2007. He was on sabbatical leave at the American University of Sharjah, Sharjah, United Arab Emirates, from 2007 to 2008, and a Senior Research Fellow with the Academy of Finland, Helsinki, Finland, from 1997 to 1998 and in 2008. He is the Co-Founder and Past CEO with SuviSoft Oy, Ltd., Tampere. From 1995 to 1998, he was a Professor with the Department of Information Technology, Pori School of Technology and Economics, Pori, Finland, and from 1997 to 1998 he was a Senior Research Scientist with the Academy of Finland. From 1994 to 1995, he was an Associate Professor with the Signal Processing Laboratory, Tampere University of Technology. From 1990 to 1993, he was a Senior Research Scientist with the Research Institute for Information Technology, Tampere. His current research interests include multimedia content-based analysis, indexing and retrieval, nonlinear signal and image processing and analysis, and video processing and coding.

Jarmo Takala (SM'02) received the M.Sc. (Distinction) and Dr.Tech. degrees from the Tampere University of Technology (TUT), Tampere, Finland, in 1987 and 1999, respectively.

From 1992 to 1996, he was a Research Scientist with VTT-Automation, Tampere. Between 1995 and 1996, he was a Senior Research Engineer with the Nokia Research Center, Tampere. From 1996 to 1999, he was a Researcher with TUT. Currently, he is a Professor with the Department of Computer Systems, TUT. His current research interests include circuit techniques, parallel structures, and design methodologies for digital signal processing systems.